Published in final edited form as:
Methods. 2009 March ; 47(3): 206–213. doi:10.1016/j.ymeth.2008.09.002.

AFM for analysis of structure and dynamics of DNA and protein-DNA complexes

Yuri L. Lyubchenko* and **Luda S. Shlyakhtenko**
Department of Pharmaceutical sciences, University of Nebraska medical Center, Omaha, NE 68198-6025

Abstract

This paper describes protocols for studies of structure and dynamics of DNA and protein-DNA complexes with AFM utilizing the surface chemistry approach. The necessary specifics for the preparation of functionalized surfaces and AFM probes with the use of silanes and silatranes, including the protocols for synthesis of silatranes are provided. The methodology of studies of local and global conformations DNA with the major focus on the time-lapse imaging of DNA in aqueous solutions is illustrated by the study of dynamics of Holliday junctions including branch migration. The analysis of nucleosome dynamics is selected as an example to illustrate the application of the time-lapse AFM to studies of dynamics of protein-DNA complexes. The force spectroscopy is the modality of AFM with a great importance to various fields of biomedical studies. The AFM force spectroscopy approach for studies of specific protein-DNA complexes is illustrated by the data on analysis of dynamics of synaptic SfiI-DNA complexes. When necessary, additional specifics are added to the corresponding example.

Keywords

Atomic force microscopy (AFM); Force microscopy; DNA dynamics; Local DNA structures; Holliday junctions; DNA–protein interactions; Protein–protein interactions; Single-molecule techniques; Solution time lapse imaging

1. Introduction

Single molecule biophysics technologies due to their capability to detect transient states of molecules and biomolecular complexes are the methods of choice for studies DNA structure and dynamics. Atomic forced microscopy (AFM) is one of these methods. A unique feature of this instrument is its capability to operate in two different modalities, topographic imaging and measuring of intermolecular interactions. AFM was also successfully applied to studies of nucleic acids. Part of this success is due to the development of reliable sample preparation procedures. Several such methods were developed simultaneously in a number of laboratories (1–10). A major feature of these methods is the use of a specially prepared surface that holds (usually electrostatically) the sample in place during scanning. We used aminosilanes (10–

*Corresponding Author: Yuri L. Lyubchenko, Department of Pharmaceutical Sciences, College of Pharmacy, COP 1012, University of Nebraska Medical Center, 986025 Nebraska Medical Center, Omaha, NE 68198-6025, 402-559-1971 (office), 402-559-9543 (fax), E-Mail 1: ylyubchenko@unmc.edu.

15) and silatranes (16–22) to functionalize the mica surface with amine groups. The major advantage of these sample preparation procedures is that they work under a wide variety of ionic conditions, pH and over a wide range of temperatures. These characteristics of functionalized mica allowed us to image nucleic acids (DNA, dsRNA, kDNA) and nucleoprotein complexes of different types (reviewed in (10,13,20)). Once prepared, samples are stable and do not absorb any contaminants for weeks with minimal precautions for storing. An important property of silatrane, such as the possibility to synthesize functionalized silatranes capable of bringing to the surface a target group including chemically reactive group, is a unique property of silatranes, allowing to prepare the surfaces with desirable characteristics. The latter property was critical for routine and reliable immobilization of the sample for AFM force spectroscopy (23). This paper outlines specifics for the preparation of surfaces, samples for AFM studies including the time lapse AFM and AFM force spectroscopy. A few examples illustrating the advantages of the described techniques for the study of DNA structure and dynamics analysis are provided. However, this is a short list. In fact, the APS-mica methodology has been used in the AFM topographic studies of alternative DNA structures such as cruciforms, three-way junctions, open DNA regions (see reviews (20,24) and references therein) and various protein-DNA complexes (25–30). In addition, the silatrane chemistry including APS-mica methodology was used in numerous topographic and the force spectroscopy studies in the area of protein misfolding and aggregation (22,31–39).

2. Experimental design

2.1. Materials

Chemicals—Commercially available 3-aminopropyltriethoxy silane (e.g., Fluka, Chemika-BioChemika, Switzerland, Aldrich, USA, United Chemical Technology, USA) and N,N-diisopropylethylamine (Aldrich, Sigma). It is recommended to redistill APTES and store under argon.

Mica substrate—Any type of commercially available mica sheets (green or ruby mica). Asheville-Schoonmaker Mica Co (Newport News, VA) supplies with thick and large (more than 5×7 cm) sheets suitable for making the substrates of different sizes.

Water—Double glass distilled or deionized water filtered through 0.5 μm filter.

2.2. Functionalization of mica with 3-aminopropyltriethoxy silane (AP-mica preparation)

The protocol below describes the methodology for the preparation of positively charged mica surface provided by covalent binding of APTES to mica surface.

Place two plastic caps (cut them from regular 1.5 ml plastic tubes) on the bottom of 2 l desiccators and vacuum it with a regular vacuum pump and fill with argon. Cleave mica sheets (approx. 5×5 cm) to make them as thin as 0.1–0.05 mm and mount at the top of the desiccators. Place 30 μl of APTES into one plastic cap and 10 μl of N,N-diisopropylethylamine (Aldrich) into another cap and allow the reaction to proceed for 1–2 hours. After that remove the cap with APTES and purge argon for 2 min. Leave the sheets for 1–2 days in the desiccator to cure; AP-mica is ready for the sample deposition after that. This procedure allows one to obtain a weak cationic surface with rather uniform distribution of the charge. Dry argon atmosphere is crucial for obtaining the substrates for AFM studies and for storage of the substrate. Allow the gas to flow while you open the desiccator. With these precautions the AP-mica substrates retain their activity for several weeks.

2.3. Synthesis of 1-(3-aminopropyl)silatrane (APS)

APS is not commercially available, but can be synthesized with use of rather simple equipment. A catalytic amount of sodium metal (5 mg) is added to 15.0 mL (16.8 g, 0.11 mol) of triethanolamine (Aldrich) in a 250 mL round-bottom flask under argon or nitrogen atmosphere and allowed to form a solution. A rubber balloon is then attached to the flask via a rubber septum and a needle to allow hydrogen to escape without building up pressure. Moderate heat (up to 100°C) can be applied to accelerate the process, but the mixture should be allowed to cool to room temperature before the next step. An equivalent amount of (3-aminopropyl) triethoxysilane (26.4 mL or 25.0 g, 0.11 mol) is added to the mixture, then the flask is placed into a 60° C water bath and connected to the vacuum line to absorb ethanol released in the reaction. This reaction can be simply performed on a rotary evaporator. At the end of the reaction, the mixture loses approximately 17 g of ethanol and is turned into a solid. This process can take more than 24 hr, but mechanical or occasional manual stirring can reduce time to 1–2 hr. Evaporation at the end with 150 mL of xylenes at 60° can also accelerate the process and help crystallization. Vacuum-dried APS obtained by this method can be used directly for AFM, or for better results and higher stability, the product can be purified by crystallization. Minute amounts of sodium hydroxide in the product does not practically affect the performance of the reagent, or change the pH of stock solutions of APS used for AFM. Recrystallization from xylenes provides 20 g (80% yield) of colorless solid powder. The synthesized APS has the following characteristics: m.p. 91–94°C (open capillary tube); m.p. 87.2–87.9°C (sealed capillary tube). ^{1}H NMR (DMSO-d_6), ppm: 0.08–0.14 (2H, m, $SiCH_2$); 1.1 (2H, br. s, NH_2); 1.28–1.37 (2H, m, CH_2); 2.37 (2H, t J = 7.2 Hz, NCH_2); 2.77 (6H, t J = 5.9 Hz, NCH_2); 3.59 (6H, t J = 5.9 Hz, OCH_2).

2.4. Mica functionalization with APS

Figure 1 schematically illustrates the reaction of APS with mica. Prepare 50 mM APS stock solution in water and store it in refrigerator. The shelf life of the stock solution is not less than 6 months. Prepare working APS solution for mica modification dissolving the stock solution in 1:300 ratio in water; it can be stored at room temperature for several days. Cleave mica sheets of needed sizes (typically 1×3 cm) to make them as thin as 0.05–0.1 mm, place them in appropriate plastic tubes and pour working APS solution to cover the mica sheet and leave on the bench for 30 min. Remove the mica sheets wash with deionized water and dry them under Argon stream. The strips are ready for the sample preparation. Note, however, as prepared, the APS mica sheets can be stored under Argon for several days.

2.5. Sample preparation for AFM imaging in air

Two procedures are described. AP-mica is mentioned in the protocols below, in the droplet and immersion procedures, however the same protocol is also applied for APS-mica. The first procedure is attractive due to the use of small amount of the sample, whereas the immersion procedure is recommended for procedures requiring the control of environmental conditions such as temperature, pH and salt concentration.

2.5.1. The Droplet Procedure—Prepare the solution of the sample (DNA, RNA, protein-DNA complex) in appropriate buffer. DNA concentration should be between 0.1 –0.01 μg/ml depending on the size of the molecules. Place 5–10 μl of the solution in the middle of AP-mica substrate (usually 1×1 cm squares) for 2–3 min. Rinse the surface thoroughly with water (2–3 ml per sample) to remove all buffer components. 5ml plastic syringe is very useful for rinsing. Attach an appropriate plastic tip instead of metal needle. Dry the sample by blowing with clean argon gas. The sample is ready for imaging. Store the samples in vacuum cabinets or desiccators filled with argon.

2.5.2. The Immersion procedure—This procedure is recommended if the deposition should be performed at strictly controlled temperature conditions (0°C or elevated temperatures) and long-time incubations. Preincubate the DNA solution for 10–20 min to allow the temperature to equilibrate. Immerse a piece of AP-mica into the vials and leave it for 10–20 min to allow the samples to adsorb to the surface. Remove the specimen, rinse with water thoroughly and dry under the argon flow. The sample is ready for imaging. The samples can be stored in vacuum cabinet or under argon.

2.6. Procedure for AFM imaging in air

The procedure for imaging in air is straightforward: mount the sample and start approaching. Although both contact and intermittent (tapping) modes can be used, the latter is preferable and allows one to get images of DNA and DNA-protein complexes routinely. Any types of probes designed for non-contact imaging can be used. NanoProbe TESP tips (Digital Instruments, Inc.) or Olympus and conical sharp silicon probes of K-TEK International (Portland, OR) work well. Typical tapping frequency of 240–380 KHz; scanning rate of 1.5–2.5 Hz allows one to obtain stable images.

2.7. Procedures for imaging in solution

The capability of AFM to perform scanning in liquid is its most attractive feature for numerous biological applications allowing imaging at conditions close to physiological ones. In addition, this mode of imaging permits one to eliminate undesirable resolution-limiting capillary effect typical for imaging in air (e.g., (8,40,41)). As a result, images of DNA filaments as thin as ~3 nm were obtained in water solutions (42) and helical periodicity was observed when dried DNA samples were imaged in propanol (11). In addition to APS-mica, our previously developed procedure with the use of AP-mica can be used as a substrate for imaging in liquid (10); note that the first images of DNA in fully hydrated state were obtained by the use of AP-mica (11). This type of imaging is recommended in cases when dynamics is studied. The following procedure is described for the use of MultiMode AFM (Veeco, Santa Barbara, CA) and can be easily adapted for other systems. Install an appropriate tip in the holder designed for imaging in liquid (fluid cell). Use Si_3N_4 big triangle with thick legs or small triangle with thin legs cantilevers (42). Mount the AP –mica or APS mica sheet on the stage of the microscope. Mica pieces of 1cm × 1cm are sufficient for MultiMode AFM design of fluid cell. Attach the head of the microscope with installed fluid cell and make appropriate adjustments of the microscope. Approach the sample to the tip manually, leaving ~50–100 μm gap between the tip and the surface. This gap is sufficient to inject ~50 μl of the sample. Allow the microscope to approach the sample and to engage the tip. Adjust the values for the set point voltage and drive amplitude to improve the quality of images and start the data acquisition using the continuous mode scanning. The best resonance frequencies are usually around 6–9 kHz. APS modified mica also can be used in MFP 3D instrument (Asylum Research, Santa Barbara, CA). For that, the piece of mica should be glued to the glass slide first and then modified as described above with APS solution.

2.8. AFM force spectroscopy

This section outlines specifics for the immobilization of molecules utilizing maleimide silatrane (MAS) methodology (43), the suitability of which has been proven in a number of single molecule experiments including AFM force spectroscopy (22,43–45).

The immobilization chemistry is shown in Fig. 2. A freshly cleaved mica surface (cartoon **1**) is treated with an aqueous solution of maleimide silatrane (MAS, **2)** for several minutes and then rinsed, leading to a surface containing immobilized maleimide units as depicted in cartoon **3**. Surface **3** is then treated with a buffered solution containing the solution of thiol-modified

DNA. The terminal thiol group covalently adds to the maleimide units on the surface leading to the immobilized DNA as shown in cartoon **4**.

Thiol group was incorporated into DNA during a standard chemical synthesis. Specifics for the preparation and purification of DNA can be found in (45). To reduce protected thiol groups of the oligonucleotides, the duplexes were treated with 10 mM buffered solution (10 mM HEPES, 50 mM NaCl, pH 7.0) of TCEP-hydrochloride (Tris(2-carboxyethyl)phosphine) at 25°C for 10 min. Silicon nitride (Si_3N_4) or MLCT AFM tips were initially washed in ethanol by immersion for 30 min and then activated by UV treatment for 30 min t. Activated tips and freshly cleaved mica surface were treated with 167 μM solution of maleimide-silatrane for 3 hours followed by rinsing with deionized water. Maleimide functionalized AFM tips and mica were incubated for 1 hour respectively in 10 μM and 80 μM of double stranded DNA. After washing with HEPES buffer solution (10 mM HEPES, 50 mM NaCl, pH 7.0), unreacted maleimide moieties were quenched with buffered 10 mM β-mercaptoethanol solution by 10 min treatment at room temperature. The modified tips and mica were washed with 10 mM HEPES, 50 mM NaCl, pH 7.0 and stored in the same buffer until use.

3. Specific AFM experiments with the use of functionalized surfaces

3.1. AFM imaging with the use of functionalized surfaces

The procedure for the preparation of samples with the use of functionalized AP-mica or APS-mica procedures is straightforward. The sample is placed onto the surface to allow the sample to diffuse to the surface and bind. After that, the sample is rinsed with water, dried with a clean gas and placed on the microscope stage for imaging. Figure 3 shows typical images obtained with the use of described protocols. We were able to image as well such an alternative DNA structure as supercoil stabilized cruciforms (46–48). The following features of AP- and APS-mica protocol were critical in reliable and reproducible detection of these dynamic structures.

1. The samples can be deposited in a wide range of ionic conditions, temperatures and pH.
2. No divalent cations are needed for the sample binding to the surface.
3. The substrate is stable and retains the binding activity during several days after the preparation.
4. The samples deposited on the substrates are stable and do not accumulate impurities during several months with minimal precautions for the sample storage.

The following issue related to the effect of the surface on the DNA conformation should be taken into a consideration. Deposition of DNA molecules on a surface certainly leads to distortion of its structure, but the extent of such distortion depends on the physical and chemical characteristics of the surface and the DNA-surface interactions. Quite popular methods utilizing the use of divalent cations work very well for imaging of linear DNA (1,49,50). At the same time, the use of a modified Mg-assisted technique the images of supercoiled DNA appear with large loops between the very tightly twisted segments of the plectonemic superhelix was a typical feature of such images (51–55). Such large loops should not present in DNA in solution and they are not appear on the computer simulated images (56); therefore the appearances of large loops in supercoiled DNA are probably induced by the immobilization procedure. The use of functionalized mica allowed us to eliminate or at least to minimize above mentioned problems and to obtain the images of supercoiled DNA (42) fully consistent with the data obtained in solution (57) and the predictions of theoretical analysis for the conformations of supercoiled DNA (56). In addition, supercoiled DNA in low salt buffer, but in the presence of Mg^{2+} cations are observed as tightly interwound plectonemic molecules

(19,42). This observation is in perfect agreement with data in solution (58), suggesting that the charge neutralization effect of Mg^{2+} cations is much stronger than that of monovalent cations.

Altogether, these data further warrant the application of the functionalized mica techniques to studies of global DNA conformations and the structure and dynamics of negative DNA supercoiling, which is a natural state of DNA at physiological conditions and within cells in particular. Local DNA structures are very labile and dynamic, so such conditions as ionic strength and pH are critical for their visualization. Furthermore, our AFM study revealed the interplay between the conformational transition of a cruciform and the global conformation of supercoiled DNA can be a molecular trigger for the slithering of DNA chains, the process that facilitates communication between distant sites in the molecule (24,48). Note that both AP- and APS-mica have very similar characteristics in terms of the surface smoothness, holding the sample on the surface provided and the high reproducibility of the results. Both surfaces were very useful for studies of protein-DNA complexes and specifics for these experiments can be found in a number of papers (25–28,59,60).

3.2. AFM imaging in aqueous solutions

Time-lapse imaging mode is one of the attractive modes of topographic AFM applications. In the pioneering work (61), AFM was applied to the imaging the fibrin self assembly. In the series of works from the group of Bustamante, AFM was applied to the observation of RNA polymerase movement along DNA (8,9,62–64). We used time lapse imaging and AP-mica methodology for studies dynamics of local and global dynamics of supercoiled DNA with the focus on structural dynamics of cruciforms (42,47). However, for the experiments in aqueous solutions APS-mica, there appears to be a better substrate than AP-mica. We observed that the APS mica surface remains smooth during experiments in liquid, rendering APS-mica superior to AP-mica (18). Controlling the surface density of amines is another important advantage of the APS mica method for the time-lapse AFM imaging experiments. These two features were critical, allowing single molecule AFM detection of the extensive dynamics of three-way DNA junctions (16), observations consistent with our earlier DNA cyclization studies in solution (65,66). The observation of the H-to-B- form transition (18,24) is another example. The results on direct visualization of recombination DNA dynamics enabling us to test the models for branch migration (20,67) along with visualization of dynamics of nucleosomes are briefly described in subsections below.

3.2.1. Dynamics of Holliday junctions and branch migration—In time-lapse AFM experiments, the sample was injected into an AFM flow cell mounted on APS-mica and imaged with an AFM continuously without drying the sample. A selected area with unambiguously identified Holliday junctions (HJs) was scanned continuously and the buffer change was performed without interruption of the scanning. The results for one such a time-lapse experiment are shown in Fig. 4. The arms subsequently move to an extended conformation (frame 9) followed by branch migration (12–13), resulting in the dissociation of the molecule into two linear strands as imaged in frame 13. A complete data set illustrated dynamics of the HJ and branch migration for this and other molecules shown as movies can be viewed in the supplement to paper (67). Quantitative analysis of the time-lapse data led us to conclude that branch migration requires unfolding of HJ whereas folding of the junction into conformations with antiparallel or parallel orientation of exchanging arms terminates branch migration.

Time lapse AFM with the use of APS-mica was recently applied to the analysis of the role of DNA supercoiling on the structure and dynamics of Holliday junctions (cruciforms) (68). The results of this analysis showed that the geometry of cruciform is primarily governed by the DNA supercoiling. DNA supercoiling shifts equilibrium between folded and unfolded conformations of cruciform towards the folded one with the parallel orientation of the DNA

helical strands rather than the antiparallel configuration typically observed in synthetic Holliday junctions. The effect of DNA supercoiling is enhanced in the presence of cations. These findings provide additional support for the role of DNA supercoiling in the structure and dynamics of Holliday junctions (cruciforms).

3.2.2. Structure and dynamics of nucleosomes—We have shown earlier that AP-mica is appropriate substrate for imaging of chromatin and were able to get the filaments with a clear-cut bead-on-spring morphology (25). Concatemeric sea urchin 5S rDNA array was used as a template, but the images did not reveal a clear periodicity. However, the analysis showed that the positions of nucleosomes were not random, suggesting that the chromatin structure is dynamic. The dynamic feature can be observed with the use of the simplest chromatin system, nucleosome core particle (NCP) in which DNA is slightly longer than is needed for wrapping around the histone core. Figure 6 shows the AFM image of the NCP system assembled on 352 bp DNA template, containing the most stable for histone octamer binding sequence (69). The NCPs consisting of bright blobs (nucleosome) with DNA arms not involved into wrapping are seen all over the scan. Importantly, this sample was prepared by the deposition of the NCP sample without fixation with glutaraldehyde typically used for electron microscopy studies, suggesting that the AFM procedure is gentle enough to preserve the NCP intact. Quantitative analysis of the NCP images allows one to calculate such an important parameter of NCP's as the number of DNA turns around the histone cores. For NCPs marked as 1, 2 and 3 (Fig. 5) these values are 1.7, 1.4 and 1 turns respectively. Such a broad variability of the wrapping value is an indirect indication of spontaneous dynamics of nucleosomes.

What are the pathways for such unwrapping? Does the core particle roll along the DNA template like a wheel or do each of the arms dissociate relatively independently? The models for the dynamics of NCP have been proposed (70) but never been tested. Time-lapse AFM would be an appropriate method in direct imaging the chromatin dynamics and testing these models. For experiments in liquid the NCP sample in buffer containing in 10 mM Tris-HCl (pH 7.5) and 4 mM $MgCl_2$, was injected directly into flow cell without drying. Images were acquired by using NanoScope IIId system (Veeco/Digital Instruments, Santa Barbara, CA) operating in tapping mode in liquid. NP-Probes (NP- Veeco/Digital Instruments, Inc.), with a spring constant 0.06 N/m and resonant frequency between 5–10 kHz were used. The continued scanning over the selected area (about 800×800nm image size) was performed to follow the dynamics of NCPs. The result of one of the time-lapse experiments for a selected NCP is shown on Fig. 6a as a subset of 7 consecutive frames. As it is seen from the images, this particular NCP, is initially quite compact with about two turns of DNA wrapped around nucleosome core (frames 51 and 52). The following frames (53–55) show that over time DNA spontaneously unwraps from the histone core and the particle in frame 54 has only about 1 turn left around the histone core. Additional unwrapping occurs later, so the next image (frame 55) corresponds to fully unwrapped complex that is loosely bound, so the core dissociates and leaves the area of observation (frame 57). The unwrapping process of the NCP in each frame was analyzed quantitatively by measuring the length of DNA arms, the angle between DNA arms and the size of the nucleosome core. These data are shown as graphs in Figs. 6B. The graph shows that the NCP dynamics is accompanied by the elongation of both arms of DNA and the decrease of the blob size. All these measurements are consistent with the NCP unwrapping process that follows the model with the independent unwrapping of each arm. We did not observe rolling of the core along the DNA template that may be a feature of the template sequence that selected by the highest affinity for the core. Similar study with the use of other sequence may clarify this issue.

Such extensive long time observations were possible due to finding the conditions at which segmental DNA mobility was low enough to allow DNA adopt various local conformations permitting the protein to move. However, further decreasing the surface-DNA interaction to

facilitate DNA mobility typically leads to sweeping the molecule away from the scan area by a scanning tip. Thus, the time lapse imaging protocol should satisfy two conflicting conditions – the molecule should be sufficiently mobile to allow observation of dynamic processes and at the same time the molecule should remain within the observation area during the entire imaging experiment. Although time lapse AFM is very attractive feature allowing to evaluate the system dynamics, one should keep in mind that the requirement for the system to be bound to the surface even intermittently influences the dynamics of the system. Therefore, time lapse AFM experiments provide the propensity of the system to adopt various conformations, but do not allow one to extract the time for such a dynamics. Recent advances in AFM technology that have led to development of the system capable of scanning 1000 times faster than traditional instruments (71–74) alleviating the problem with sample immobilization. However, the limitation with the need of the sample to be bound to the surface for the AFM imaging does not eliminate the problem with evaluation of system dynamics times.

3.3. AFM force spectroscopy: Stability and dynamics of synaptic DNA-protein complexes

AFM force spectroscopy allowing measurements of intermolecular interaction as well as intramolecular stability is the area of AFM application with fast growing demand. In this mode, the AFM measures the mechanical stability of the system positioned between the surface and AFM tip. Covalent attachment of the system at a well defined anchoring point is required for the force pulling experiments. We have shown that functionalized surfaces open prospects for immobilizing the system in fast, efficient and reproducible fashion (22,23,38,44,45,75–79). The most promising is the approach with the use of silatranes with specific reactive groups allowing anchoring the molecule via formation of covalent bonds. The example below illustrates the immobilization approach utilizing maleimide silatrane capable of binding thiol-containing molecules.

Our AFM topographic studies of the complex formed by SfiI restriction enzyme and DNA revealed a number of important structural characteristics of this system, suggesting interesting dynamic properties of this system. We have developed single molecule AFM force spectroscopy approach enabling one to measure the stability of site-specific protein-DNA complexes involving the interaction of two DNA sites performed by a specific complex (45). The experimental setup is shown schematically in Fig. 7. The identical DNA duplexes containing SfiI recognition sites (shown as two parallel red thick lines) are covalently attached to the AFM substrate and tip via flexible linker (zigzag green lines, section A). The synaptic complex between the two duplexes is formed by SfiI when the duplexes are in the proximity to each other and SfiI (blue tetrameric oval) binds to them (section B). The complex was formed by the protein present in the solution. Upon retraction of the tip, the flexible linkers are stretched (section C) and the complex is ruptured when the stretching limit is achieved (section D).

The stability of the synaptic complex formed by the enzyme and two DNA duplexes was probed in a series of approach-retraction cycles during which the force distance curved are captured. A typical force-distance curve obtained using the experimental setup for studying the synaptic complex schematically represented by Figure 7A–D is shown in Figure 8. An adhesive peak at the beginning of the force curve (section B of the force curve) is accompanied by a force extension curve (section C) corresponding to the stretching of polymer linkers, followed by a rupture of the synaptic complexes event (section D). A series of control experiments allowed us to justify this assignment (45). The maleimide silatrane immobilization strategy allowed us to determine the dissociation rate (k_{off}) with a high accuracy due to the possibility to acquire a large set of the data. For example, the DFS experiments performed with two different sequences within the middle part of the DNA recognition region revealed the sequence-dependent difference in the stability of synaptic complex that correlated with the effect of the sequence on the SfiI enzymatic activity (80). Note again that the key in these experiments was

the high yield of rupture events rupture events ca.10–20% vs. ca. 1% for multistep procedures, e.g., (81).

4. Conclusions

The preparation of the AFM substrates and probes with various surface characteristics is a fundamental issue for reliable and routine use of AFM for studies nucleic acids and their complexes with protein. In this paper, we illustrated the capabilities of the approach utilizing silane and recently developed silatrane surface chemistries. The latter was essential in facilitating the use of AFM in both imaging and force spectroscopy modes. Strong polyanionic properties of nucleic acids were central to the development of reliable methods of attaching them to substrates, which is necessary for high-resolution AFM imaging. However, attachment of the molecule, for example, a protein interaction with DNA at selected points may require for such applications as time-lapse imaging. We believe that further progress in the silatrane surface chemistry allowing controlled immobilization of specific groups of the proteins with minimal interfering with their activity will further facilitate such applications as time lapse AFM imaging in the fast scanning mode and AFM force spectroscopy applications.

Acknowledgements

We thank A. Portillo for proofreading of the manuscript. This work was supported in part by National Institutes of Health Grants GM 062235, the National Science Foundation (0615590 and 0701892) and Nebraska Research Initiative (NRI).

References

1. Bustamante C, Vesenka J, Tang CL, Rees W, Guthold M, Keller R. Biochemistry 1992;31:22–6. [PubMed: 1310032]
2. Yang J, Takeyasu K, Shao Z. FEBS Lett 1992;301:173–6. [PubMed: 1314740]
3. Vesenka J, Guthold M, Tang CL, Keller D, Delaine E, Bustamante C. Ultramicroscopy 1992;42–44 (Pt B):1243–9.
4. Lyubchenko YL, Gall AA, Shlyakhtenko LS, Harrington RE, Jacobs BL, Oden PI, Lindsay SM. J Biomol Struct Dyn 1992;10:589–606. [PubMed: 1492926]
5. Allen MJ, Dong XF, O'Neill TE, Yau P, Kowalczykowski SC, Gatewood J, Balhorn R, Bradbury EM. Biochemistry 1993;32:8390–6. [PubMed: 8357790]
6. Hegner M, Wagner P, Semenza G. FEBS Lett 1993;336:452–6. [PubMed: 8282109]
7. Mou J, Czajkowsky DM, Zhang Y, Shao Z. FEBS Lett 1995;371:279–82. [PubMed: 7556610]
8. Bustamante C, Erie D, Keller D. Curr Opinion in Struct Biol 1994;4:750–60.
9. Bustamante C, Rivetti C, Keller DJ. Curr Opin Struct Biol 1997;7:709–16. [PubMed: 9345631]
10. Lyubchenko YL, Gall AA, Shlyakhtenko LS. Methods Mol Biol 2001;148:569–78. [PubMed: 11357614]
11. Lyubchenko Y, Shlyakhtenko L, Harrington R, Oden P, Lindsay S. Proc Natl Acad Sci U S A 1993;90:2137–40. [PubMed: 8460119]
12. Lyubchenko YL, Oden PI, Lampner D, Lindsay SM, Dunker KA. Nucleic Acids Res 1993;21:1117–23. [PubMed: 8464697]
13. Lyubchenko YL, Jacobs BL, Lindsay SM, Stasiak A. Scanning Microsc 1995;9:705–24. [PubMed: 7501986]discussion 24–7
14. Lyubchenko YL, Blankenship RE, Gall AA, Lindsay SM, Thiemann O, Simpson L, Shlyakhtenko LS. Scanning Microsc Suppl 1996;10:97–107. [PubMed: 9601533]
15. Lyubchenko, YL.; Lindsay, SM. Procedures in Scanning Probe Microscopy. Engel, A., editor. Wiley & Sons, Ltd; New York, Toronto: 1998. p. 493-96.
16. Shlyakhtenko LS, Potaman VN, Sinden RR, Gall AA, Lyubchenko YL. Nucleic Acids Res 2000;28:3472–7. [PubMed: 10982865]

17. Tiner WJ Sr, Potaman VN, Sinden RR, Lyubchenko YL. J Mol Biol 2001;314:353–7. [PubMed: 11846549]
18. Shlyakhtenko LS, Gall AA, Filonov A, Cerovac Z, Lushnikov A, Lyubchenko YL. Ultramicroscopy 2003;97:279–87. [PubMed: 12801681]
19. Shlyakhtenko LS, Miloseska L, Potaman VN, Sinden RR, Lyubchenko YL. Ultramicroscopy 2003;97:263–70. [PubMed: 12801679]
20. Lyubchenko YL. Cell Biochem Biophys 2004;41:75–98. [PubMed: 15371641]
21. Pavlicek JW, Oussatcheva EA, Sinden RR, Potaman VN, Sankey OF, Lyubchenko YL. Biochemistry 2004;43:10664–8. [PubMed: 15311927]
22. Lyubchenko YL, Sherman S, Shlyakhtenko LS, Uversky VN. J Cell Biochem 2006;99:53–70.
23. Riener CK, Stroh CM, Ebner A, Gall AA, Klampfl C, Romanin C, Lyubchenko YL, Hinterdorfer P, Gruber HJ. Analytica Chimica Acta 2003;479:59–75.
24. Lyubchenko YL, Shlyakhtenko LS, Potaman VP, Sinden RR. Microsc Microanal 2002;8:170–71. [PubMed: 12539787]
25. Yodh JG, Woodbury N, Shlyakhtenko LS, Lyubchenko YL, Lohr D. Biochemistry 2002;41:3565–74. [PubMed: 11888272]
26. Lushnikov AY, Brown BA 2nd, Oussatcheva EA, Potaman VN, Sinden RR, Lyubchenko YL. Nucleic Acids Res 2004;32:4704–12. [PubMed: 15342791]
27. Lonskaya I, Potaman VN, Shlyakhtenko LS, Oussatcheva EA, Lyubchenko YL, Soldatenkov VA. J Biol Chem 2005;280:17076–83. [PubMed: 15737996]
28. Lushnikov AY, Potaman VN, Lyubchenko YL. Nucleic Acids Res 2006;34:e111. [PubMed: 16963492]
29. Lushnikov AY, Potaman VN, Oussatcheva EA, Sinden RR, Lyubchenko YL. Biochemistry 2006;45:152–58. [PubMed: 16388590]
30. Shlyakhtenko LS, Gilmore J, Portillo A, Tamulaitis G, Siksnys V, Lyubchenko YL. Biochemistry 2007;46:11128–36. [PubMed: 17845057]
31. Liu R, Yuan B, Emadi S, Zameer A, Schulz P, McAllister C, Lyubchenko Y, Goud G, Sierks MR. Biochemistry 2004;43:6959–67. [PubMed: 15170333]
32. Liu R, McAllister C, Lyubchenko Y, Sierks MR. Biochemistry 2004;43:9999–10007. [PubMed: 15287727]
33. Liu R, McAllister C, Lyubchenko Y, Sierks MR. J Neurosci Res 2004;75:162–71. [PubMed: 14705137]
34. Emadi S, Liu R, Yuan B, Schulz P, McAllister C, Lyubchenko Y, Messer A, Sierks MR. Biochemistry 2004;43:2871–8. [PubMed: 15005622]
35. Yamin G, Munishkina LA, Karymov MA, Lyubchenko YL, Uversky VN, Fink AL. Biochemistry 2005;44:9096–107. [PubMed: 15966733]
36. Uversky VN, Yamin G, Munishkina LA, Karymov MA, Millett IS, Doniach S, Lyubchenko YL, Fink AL. Brain Res Mol Brain Res 2005;134:84–102. [PubMed: 15790533]
37. Dahlgren PR, Karymov MA, Bankston J, Holden T, Thumfort P, Ingram VM, Lyubchenko YL. Dis Mon 2005;51:374–85. [PubMed: 16242522]
38. Uversky VN, Kabanov AV, Lyubchenko YL. J Proteome Res 2006;5:2505–22. [PubMed: 17022621]
39. Shlyakhtenko LS, Yuan B, Emadi S, Lyubchenko YL, Sierks MR. Nanomedicine 2007;3:192–7. [PubMed: 17662669]
40. Hansma HG, Hoh JH. Annu Rev Biophys Biomol Struct 1994;23:115–39. [PubMed: 7919779]
41. Lyubchenko YL, Jacobs BL, Lindsay SM, Stasiak A. Scanning Microsc 1995;9:705–24. [PubMed: 7501986]discussion 24–7
42. Lyubchenko YL, Shlyakhtenko LS. Proc Natl Acad Sci U S A 1997;94:496–501. [PubMed: 9012812]
43. Kransnoslobodtsev AV, Shlyakhtenko LS, Ukraintsev E, Zaikova TO, Keana JFW, Lyubchenko YL. Nanomedicine: Nanotechnology, Biology, and Medicine 2005;1:300–05.
44. Karymov MA, Krasnoslobodtsev AV, Lyubchenko YL. Biophys J 2007;92:3241–50. [PubMed: 17277188]

45. Krasnoslobodtsev AV, Shlyakhtenko LS, Lyubchenko YL. J Mol Biol 2007;365:1407–18. [PubMed: 17125791]
46. Shlyakhtenko LS, Potaman VN, Sinden RR, Lyubchenko YL. J Mol Biol 1998;280:61–72. [PubMed: 9653031]
47. Engel A, Lyubchenko Y, Muller D. Trends Cell Biol 1999;9:77–80. [PubMed: 10087624]
48. Shlyakhtenko LS, Hsieh P, Grigoriev M, Potaman VN, Sinden RR, Lyubchenko YL. J Mol Biol 2000;296:1169–73. [PubMed: 10698623]
49. Thundat T, Allison DP, Warmack RJ, Brown GM, Jacobson KB, Schrick JJ, Ferrell TL. Scanning Microsc 1992;6:911–8. [PubMed: 1295085]
50. Hansma HG, Laney DE, Bezanilla M, Sinsheimer RL, Hansma PK. Biophys J 1995;68:1672–7. [PubMed: 7612809]
51. Pfannschmidt C, Schaper A, Heim G, Jovin TM, Langowski J. Nucleic Acids Res 1996;24:1702–9. [PubMed: 8649989]
52. Rippe K, Mucke N, Langowski J. Nucleic Acids Res 1997;25:1736–44. [PubMed: 9108155]
53. Pfannschmidt C, Langowski J. J Mol Biol 1998;275:601–11. [PubMed: 9466934]
54. Jett SD, Cherny DI, Subramaniam V, Jovin TM. J Mol Biol 2000;299:585–92. [PubMed: 10835269]
55. Nagami F, Zuccheri G, Samori B, Kuroda R. Anal Biochem 2002;300:170–6. [PubMed: 11779108]
56. Vologodskii A, Cozzarelli NR. Biophys J 1996;70:2548–56. [PubMed: 8744294]
57. Rybenkov VV, Vologodskii AV, Cozzarelli NR. Nucleic Acids Res 1997;25:1412–8. [PubMed: 9060437]
58. Shaw SY, Wang JC. Science 1993;260:533–6. [PubMed: 8475384]
59. Potaman VN, Shlyakhtenko LS, Oussatcheva EA, Lyubchenko YL, Soldatenkov VA. J Mol Biol 2005;348:609–15. [PubMed: 15826658]
60. Shlyakhtenko LS, Gilmore J, Portillo A, Tamulaitis G, Siksnys V, Lyubchenko YL. Biochemistry 2007;46:11128–36. [PubMed: 17845057]
61. Drake B, Prater CB, Weisenhorn AL, Gould SA, Albrecht TR, Quate CF, Cannell DS, Hansma HG, Hansma PK. Science 1989;243:1586–9. [PubMed: 2928794]
62. Guthold M, Bezanilla M, Erie DA, Jenkins B, Hansma HG, Bustamante C. Proc Natl Acad Sci U S A 1994;91:12927–31. [PubMed: 7809148]
63. Bustamante C, Rivetti C. Annu Rev Biophys Biomol Struct 1996;25:395–429. [PubMed: 8800476]
64. Guthold M, Zhu X, Rivetti C, Yang G, Thomson NH, Kasas S, Hansma HG, Smith B, Hansma PK, Bustamante C. Biophys J 1999;77:2284–94. [PubMed: 10512846]
65. Shlyakhtenko LS, Appella E, Harrington RE, Kutyavin I, Lyubchenko YL. J Biomol Struct Dyn 1994;12:131–43. [PubMed: 7848563]
66. Shlyakhtenko LS, Rekesh D, Lindsay SM, Kutyavin I, Appella E, Harrington RE, Lyubchenko YL. J Biomol Struct Dyn 1994;11:1175–89. [PubMed: 7946068]
67. Lushnikov AY, Bogdanov A, Lyubchenko YL. J Biol Chem 2003;278:43130–4. [PubMed: 12949070]
68. Mikheikin AL, Lushnikov AY, Lyubchenko YL. Biochemistry 2006;45:12998–3006. [PubMed: 17059216]
69. Polach KJ, Widom J. J Mol Biol 1995;254:130–49. [PubMed: 7490738]
70. Widom J. Q Rev Biophys 2001;34:269–324. [PubMed: 11838235]
71. Ando T, Kodera N, Takai E, Maruyama D, Saito K, Toda A. Proc Natl Acad Sci U S A 2001;98:12468–72. [PubMed: 11592975]
72. Kobayashi M, Sumitomo K, Torimitsu K. Ultramicroscopy 2007;107:184–90. [PubMed: 16949754]
73. Ando T, Uchihashi T, Kodera N, Yamamoto D, Miyagi A, Taniguchi M, Yamashita H. Pflugers Arch 2008;456:211–25. [PubMed: 18157545]
74. Crampton N, Yokokawa M, Dryden DT, Edwardson JM, Rao DN, Takeyasu K, Yoshimura SH, Henderson RM. Proc Natl Acad Sci U S A 2007;104:12755–60. [PubMed: 17646654]
75. Limansky AP, Shlyakhtenko LS, Schaus S, Henderson E, Lyubchenko YL. Probe Microscopy 2002;4:1–6.
76. Kransnoslobodtsev AV, Shlyakhtenko LS, Ukraintsev E, Zaikova TO, Keana JF, Lyubchenko YL. Nanomedicine 2005;1:300–05. [PubMed: 16467913]

77. McAllister C, Karymov MA, Kawano Y, Lushnikov AY, Mikheikin A, Uversky VN, Lyubchenko YL. J Mol Biol 2005;354:1028–42. [PubMed: 16290901]

78. Wei C, Lyubchenko YL, Ghandehari H, Hanes J, Stebe KJ, Mao HQ, Haynie DT, Tomalia DA, Foldvari M, Monteiro-Riviere N, Simeonova P, Nie S, Mori H, Gilbert SP, Needham D. Nanomedicine: Nanotechnology, Biology, and Medicine 2006;2:253–63.

79. Wei C, Liu N, Xu P, Heller M, Tomalia DA, Haynie DT, Chang EH, Wang K, Lee YS, Lyubchenko YL, Bawa R, Tian R, Hanes J, Pun S, Meiners JC, Guo P. Nanomedicine 2007;3:322–31. [PubMed: 18068093]

80. Williams SA, Halford SE. Nucleic Acids Res 2001;29:1476–83. [PubMed: 11266549]

81. Ray C, Akhremitchev BB. Journal of the American Chemical Society 2005;127:14739–44. [PubMed: 16231928]

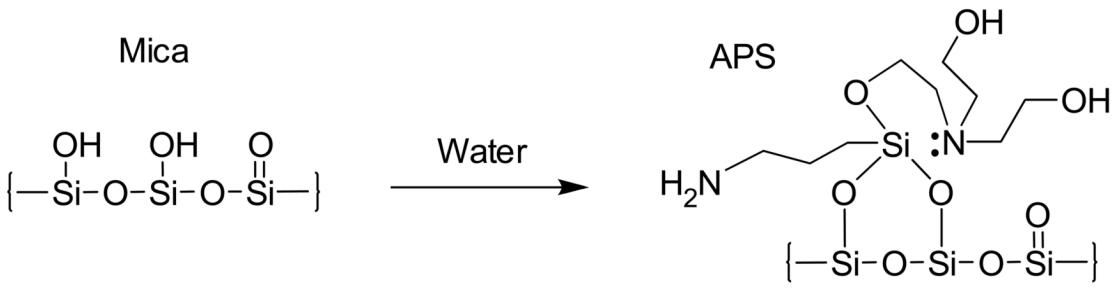

Figure 1.
Scheme for reaction of 3-aminopropylsilatrane (APS) with hydroxyl groups on a mica (silicon) surface. The initial adduct reacted with one hydroxyl group can reach with a second surface OH group forming the indicated product in a reversible equilibrium.

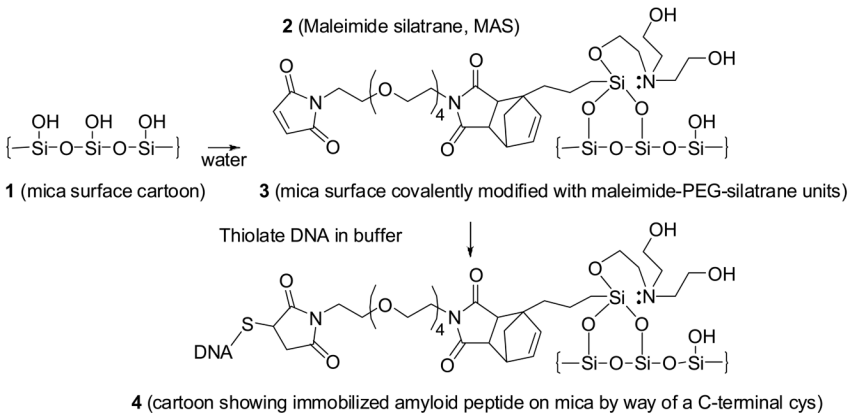

Figure 2.
Immobilization of thiolated DNA on the functionalized MAS-mica surface.

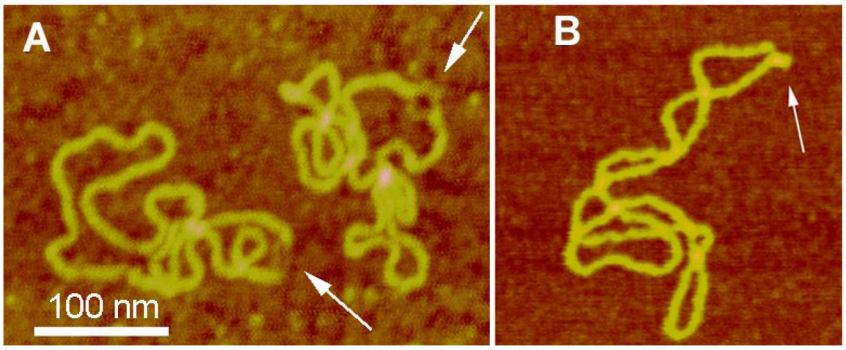

Figure 3.
AFM images of plasmid DNA with two types of alternative structures stabilized by negative supercoiling. (A) Bulges induced by denaturation at (ATTCT)29-region [1]. Open regions are indicated with arrows. (B) H-DNA appearing as a thick stem indicated with an arrow (26). The samples were obtained by deposition on APS-mica.

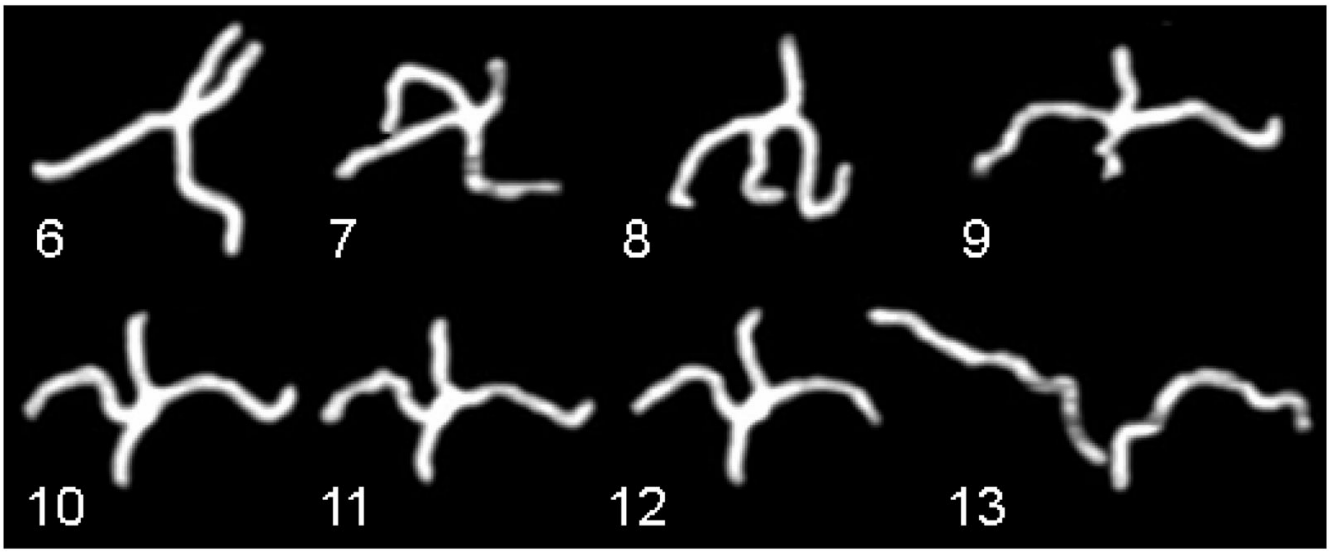

Figure 4.
Time lapse AFM images (6 to 13) illustrating unfolding (frames 6–9), dynamics of unfolded conformation (9–12) and branch migration of the Holliday junction leading to the dissociation of the junction.

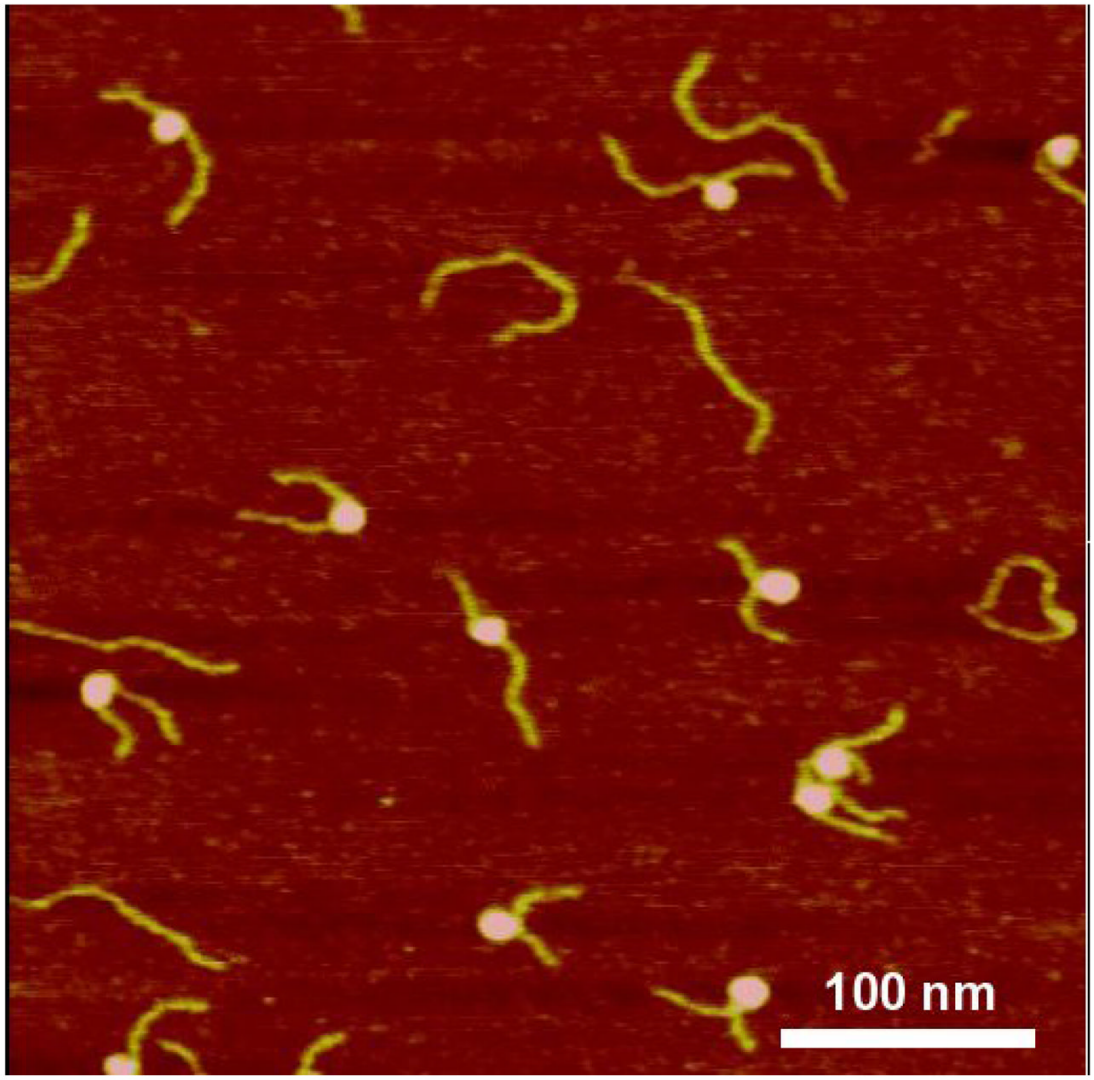

Figure 5.
AFM image of nucleosomes in air. The image represents nucleosomes with different amounts of DNA wrapped around the core particle. NCPs marked as 1, 2 and 3 have about 1.7, 1.4 and 1.0 turns of DNA wrapped around the core particle.

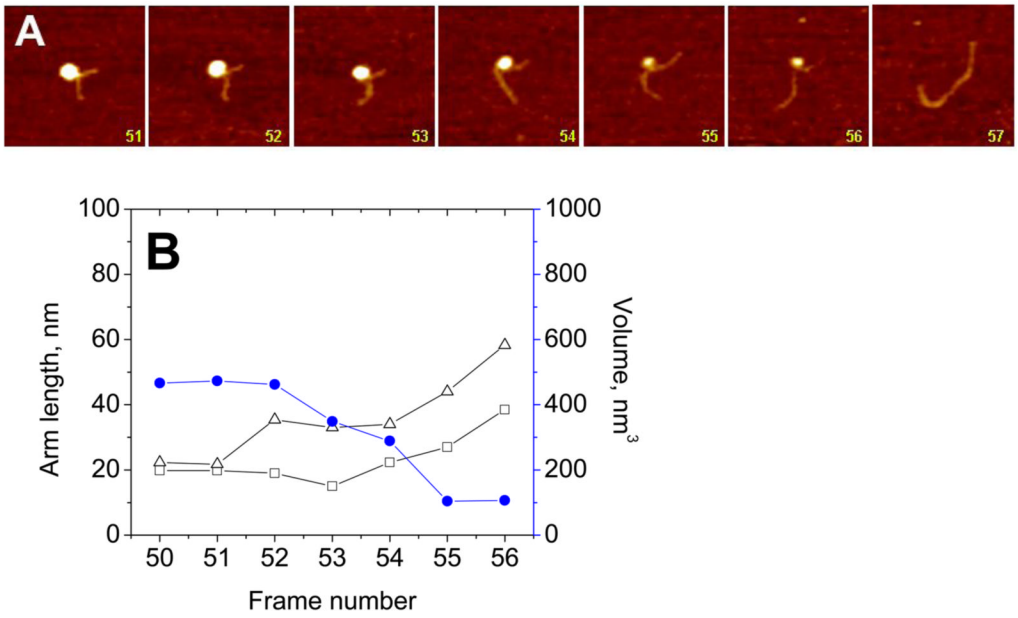

Figure 6.

(A) Time-lapse AFM experiments for 7 consecutive frames illustrating the dynamics of the nucleosome particle. The scan size is 150 nm. (B) The variability of arm length (left Y-axis, black) and protein volume (right Y-axis, blue) with the imaging frame number (X-axis).

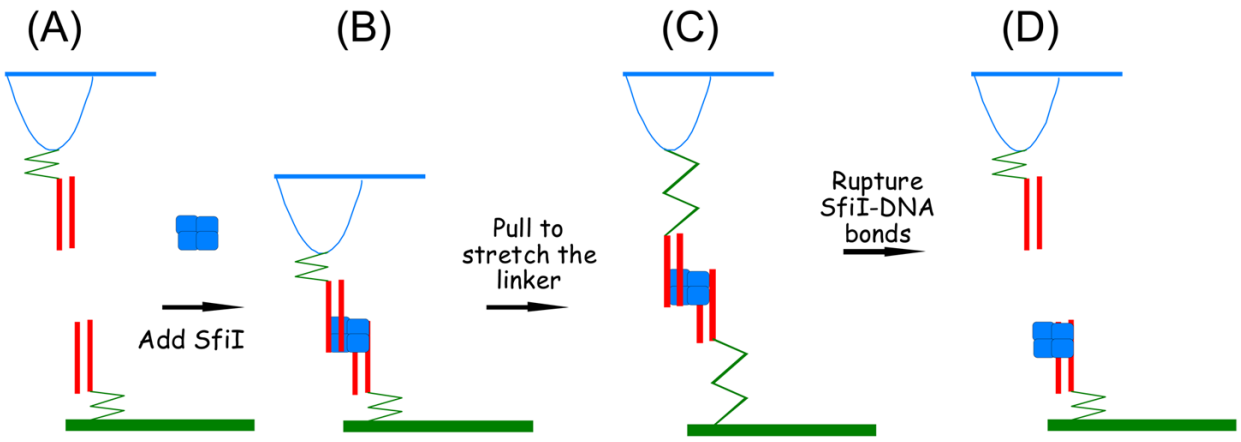

Figure 7.

Schematics for the AFM force spectroscopy experiments for measuring the strength of the synaptic complex formed by two DNA duplexes and SfiI enzyme. DNA duplexes (red parallel lines) are attached to the AFM tip and the surface via a flexible linker shown as a zigzag (A). The approach tip to the surface in the presence of the enzyme (blue box) can lead to the formation of the synaptic complex (B). Retraction of the tip away from the surface leads to stretching of the linker (C). The complex dissociates when the force reaches the rupture value for the complex. The protein can remain on one of the duplexes and dissociate later on.

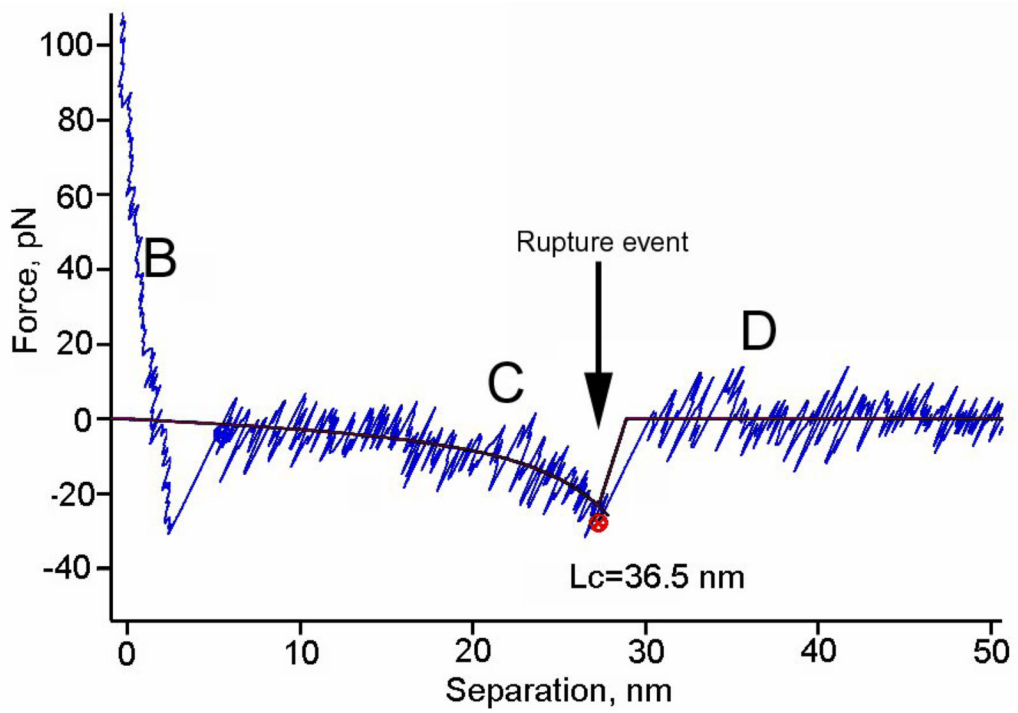

Figure 8.

A typical force-distance curve obtained for the interactions between SfiI and DNA duplex: (B) the start point of the tip retraction from surface, the force curve in this region reflects the nonspecific adhesion forces between surface and the tip; (C) the region is indicative of polymer linker stretching, this portion of the curve is fitted with worm-like chain approximation (solid red line); (D) the abrupt jump in the force curve is typical of specific bond rupture. The inset shows the rupture force histogram obtained for the synaptic complex at 150 nm/s retraction velocity (~9.5 nN/s apparent loading rate).